Development 128, 675-688 (2001)
Printed in Great Britain © The Company of Biologists Limited 2001
DEV2643

RXRα ablation in skin keratinocytes results in alopecia and epidermal alterations

Mei Li, Hideki Chiba*, Xavier Warot, Nadia Messaddeq, Christelle Gérard, Pierre Chambon‡ and Daniel Metzger

Institut de Génétique et de Biologie Moléculaire et Cellulaire, CNRS/INSERM/ULP, Collège de France, BP 163, 67404 Illkirch Cedex, France

*Present address: Sapporo Medical University, School of Medicine, Department of Pathology, South-1, West-17, Chuo-ku, SAPPORO, 060 Japan

‡Author for correspondence (e-mail: chambon@igbmc.u-strasbg.fr)

Accepted 18 December 2000; published on WWW 7 February 2001

SUMMARY

RXRα is the most abundant of the three retinoid X receptors (RXRs) in the epidermis. In this study, we have used Cre-mediated recombination to selectively disrupt the mouse gene for RXRα in epidermal and hair follicle keratinocytes. We show that RXRα is apparently dispensable for prenatal epidermal development, while it is involved in postnatal skin maturation. After the first hair pelage, mutant mice develop a progressive alopecia, histologically characterised by the destruction of hair follicle architecture and the formation of utriculi and dermal cysts in adult mice. Our results demonstrate that RXRα plays a key role in anagen initiation during the hair follicle cycle. In addition, RXRα ablation results in epidermal interfollicular hyperplasia with keratinocyte hyperproliferation and aberrant terminal differentiation, accompanied by an inflammatory reaction of the skin. Our data not only provide genetic evidence that RXRα/VDR heterodimers play a major role in controlling hair cycling, but also suggest that additional signalling pathways mediated by RXRα heterodimerised with other nuclear receptors are involved in postnatal hair follicle growth, and homeostasis of proliferation/differentiation of epidermal keratinocytes and of the skin's immune system.

Key words: Somatic mutagenesis, Cre/loxP, Keratinocytes, Epidermis, Hair follicle, Hair cycle, RXR/VDR Heterodimer, Mouse

INTRODUCTION

The skin is composed of the epidermal layer and its appendages (hair follicles) that are separated from the dermal layer by a basement membrane. The epidermis, a stratified epithelium made principally of keratinocytes, is a highly dynamic structure (Fuchs, 1997). The innermost basal layer that is attached to the basement membrane is a proliferative layer, from which keratinocytes periodically withdraw from the cell cycle and commit to terminally differentiate, while migrating into the next layers, known as the spinous and granular layers, which together represent the suprabasal layers. Terminally differentiated keratinocytes or squames, that reach the skin's surface form the cornified layer or corneum. Squamous keratinocytes are lost daily from the surface of the skin, and are continuously replaced by differentiating cells vectorially moving outward. Hair follicles that develop through a series of mesenchymal/epithelial interactions during embryogenesis are also dynamic structures. They are also principally composed of keratinocytes, and their outer root sheath (ORS) is contiguous with the epidermis. Once formed, hair follicles periodically undergo cycles of regression (catagen), rest (telogen) and growth (anagen), through which old hairs are eventually replaced by new ones (Hardy, 1992; Paus and Cotsarelis, 1999).

Ligand deprivation and pharmacological studies both in vitro with keratinocytes in culture and in vivo have indicated that the active retinoid derivatives of vitamin A (principally retinoic acid, RA) can play critical regulatory roles in growth, differentiation, and maintenance of mammalian epidermis and hair follicles (reviewed in Fisher and Voorhes, 1996; Roos et al., 1998). Retinoid signals are believed to be transduced by heterodimers between isotypes belonging to two families of nuclear receptors (NRs), the retinoic acid receptors (RARα, β and γ) and the retinoid X receptors (RXRα, β and γ) (Mangelsdorf et al., 1995; Chambon, 1996; and Refs therein). However, RXRs have also been shown to be heterodimeric partners of a number of other members of the NR superfamily (e.g. VDR and PPARs; see Giguère, 1999) that are also expressed in epidermis and hair follicles and may be involved in their development and homeostasis (see Discussion for Refs).

RXRs, and notably RXRα, which is the most abundant RXR isotype expressed in epidermis and hair follicle ORS keratinocytes (Elder et al., 1992; Fisher et al., 1994; Reichrath et al., 1995; Fisher and Voorhees, 1996), may therefore play a crucial role in epidermal and hair follicle development and maintenance. However, genetic studies aimed at establishing these physiological roles by targeted disruption (knockout) of the gene for RXRα in the mouse have failed, as RXRα knockouts resulted in embryonic lethality between day 13.5 and 16.5 (Kastner et al., 1994; Sucov et al., 1994), i.e. at the time of

epidermis and hair follicle morphogenesis (Dubrul, 1972). To circumvent this obstacle, we have now used the Cre/loxP technology (Nagy, 2000) to selectively ablate RXRα expression in epidermal and hair follicle ORS. We demonstrate that RXRα plays a crucial role in postnatal skin maturation and hair cycling, as well as in homeostasis of both epidermal keratinocyte proliferation/differentiation and of the skin's immune system.

MATERIALS AND METHODS

Transgenic lines

The pK14-Cre plasmid was constructed by cloning the blunt-ended 1 kb *Eco*RI-*Bgl*II fragment isolated from pSG-Cre (Feil et al., 1997) into the blunt-ended *Eco*RI sites of pK14-Cre-ER^{T2} (Li et al., 2000). The 4 kb K14-Cre fragments were excised from the pK14-Cre plasmid by *Not*I digestion, purified through a 10-30% sucrose gradient, and injected into C57BL/6 × SJL F1 zygotes, as described (Feil et al., 1996). The Cre transgene was detected by PCR as described (Indra et al., 1999). The floxed ROSA Cre reporter line (R26R; Soriano, 1999) was genotyped by PCR, using the primers 5′-CGCCGACGGC-ACGCTGATTG-3′ and 5′-GTTTCAATATTGGCTTCATC-3′.

Targeting vector and homologous recombination

The targeting vector, pRXRα^{L2} was constructed as follows. An 11.8 kb *Sal*I-*Spe*I genomic fragment encompassing RXRα exons 2, 3 and 4 (Clifford et al., 1996) was subcloned into the *Sal*I-*Spe*I sites of pHC1, a pBluescript II SK+ (Stratagene) derivative obtained by cloning the oligonucleotides 5′-ATCGATGTCGACCGGAC-TAGTGTAC-3′ and 5′-ACTAGTCCGGTCGACATCGATAGCT-3′ into the *Sac*I and *Kpn*I sites (pRXRαC1). The oligonucleotides 5′-CTAGATAACTTCGTATAATGTATGCTATACGAAGTTATAAG-CTTC-3′ and 5′-CTAGGAAGCTTATAACTTCGTATAGCATACA-TTATACGAAGTTAT-3′, containing a loxP site, were cloned into the *Xba*I site of pRXRαC1, resulting in pRXRαCL1. Finally, the 3 kb *Eco*RI fragment containing the tk-neo cassette and a loxP site at its 3′ end, isolated from pHR56E, was cloned into *Eco*RI site of pRXRαCL1 (Fig. 2). pHR56E was constructed by converting the *Xba*I site of pHR56 (Metzger et al., 1995) into an *Eco*RI site. The 14.3-kb *Cla*I fragment was purified on a 10-30% sucrose gradient and electroporated into P1 embryonic stem (ES) cells, as described (Dierich and Dollé, 1997). After selection with G418, 220 resistant clones were expanded. Genomic DNA was prepared from each clone, restricted with *Xba*I and analysed by Southern blotting with probe X5. Nine clones positive for homologous recombination were further analysed by a *Spe*I digest and probe X4 and *Hin*dIII digest and neomycin probes (Metzger et al., 1995). X4 and X5 correspond to 3 kb *Bam*HI-*Xba*I and 0.5 kb *Hin*dIII-*Spe*I DNA fragments, respectively, isolated from the RXRα genomic clone. Four positive ES clones were injected into C57BL/6 blastocysts, and male chimaeras derived from two of them gave germline transmission. Mutant animals derived from both lines exhibited similar phenotypes.

Genotyping of the RXRα alleles

Genomic DNA was isolated as described (Feil et al., 1996). To identify the various RXRα alleles, genomic PCR was performed with primers ZO243 (5′-TCCTTCACCAAGCACATCTG-3′) (located in exon 3) and 3′-primer ZO244 (5′-TGCAGCCCTCACAACTGTAT-3′) (located in exon 4) (L2 and (+) alleles; 700 bp and 650 bp fragments, respectively); ZO243 and UD196 (5′-CAACCTGGACTTGTCACT-TAG-3′; located in the intron between Exon 4 and 5; L– allele; 400 bp fragment) and ZO243 and RU178 (5′-ATGTTTCATAG-TTGGATATC-3′; located in the neo cassette; Kastner et al., 1994) [(–) allele; 500 bp]. For Southern blot analysis, genomic DNA was digested with *Bam*HI and hybridised with X4 probe. To quantify the excision efficiency of floxed RXRα alleles in epidermis, tail skin was treated with dispase enzyme at 4 mg/ml in PBS (Gibco-BRL) at room temperature for 1-2 hours, the epidermis was separated from the dermis and genomic DNA was extracted.

Anagen induction

20 days post-partum anaesthetised mice were subjected to depilation of dorsal hair using wax stripes (Paus et al., 1990). Skin biopsies from the mid-dorsum were taken at various days for histological analysis.

Histological and electron microscopic analysis

All skin biopsies were matched for age, sex and body sites. For 5 and 7 μm sections, skin samples were fixed in Bouin's fixative and embedded in paraffin and stained with Haematoxylin and Eosin or Haematoxylin of Harris. For 2 μm semi-thin section, skin samples were fixed in 2.5% glutaraldehyde in 0.1 M cacodylate buffer (PH7.2) (overnight at 4°C), post-fixed with 1% osmium tetroxide in cacodylate buffer for 1 hour at 4°C, dehydrated with graded concentrations of alcohol and embedded in Epon 812. 2 μm semi-thin sections were stained with toluidine blue and analysed by light microscope. 70 nm ultra-thin sections were contrasted with uranyl acetate and lead citrate, and examined with a Philips 208 electron microscope.

Histochemistry

β-Galactosidase histochemistry was performed on 10 μm-thick frozen section, stained with X-Gal (5-bromo-4-chloro-3-indolyl β-D-galactoside), or on 2 μm semi-thin sections as described (Brocard et al., 1997).

Immunofluorescence was performed on 10 μm skin cryosections. After fixation in 2% paraformaldehyde, sections were blocked in 5% NGS (normal goat serum, Vector), incubated with primary antibody (rabbit polyclonal anti-MK6 and rabbit polyclonal anti-filaggrin (Babco); mouse monoclonal anti-K10, mouse monoclonal anti-K14, and rabbit polyclonal anti-K5 (gifts from Prof. E. Brigitte Lane, Cell Structure Research Group, University of Dundee); biotin-conjugated monoclonal hamster anti-CD3, rat monoclonal anti-CD4, rat monoclonal anti-CD8, biotin-conjugated rat monoclonal anti-CD31 and biotin-conjugated monoclonal hamster anti-CD54 (PharMingen)). After washing in PBS/0.1% Tween 20, sections were incubated either with the CY3-conjugated donkey anti-rabbit, CY3-conjugated goat anti-mouse IgG antibodies or CY3-streptavidine (Jackson Immunoresearch). Counterstaining was performed with DAPI (4′, 6-diamidino-2-phenylindole dihydrochloride, Boehringer Mannheim) (Brocard et al., 1997).

For RXRα immunohistochemistry, skin samples were fixed with periodate-lysine-paraformaldehyde (Kiernan, 1990), dehydrated in graded sucrose and embedded in OCT. A 10 μm cryosection was blocked with 5% NGS, incubated with biotin-conjugated RXRα monoclonal antibody 4RX3A2 (Rochette-Egly et al., 1994), and revealed with Vectastain ABC kit (Vector) and 4-chloro-1-naphtol peroxidase substrate (Merck).

Bromodeoxyuridine (BrdU) labelling

Mice were injected subcutaneously with BrdU (50 μg per gram body weight) and sacrificed 2 hours later. Skin samples were fixed in Bouin and embedded in paraffin. 7 μm thick sections were incubated with an anti-BrdU monoclonal antibody (Boehringer Mannheim), and revealed with the Vectastain ABC kit (Vector) and peroxidase substrate DAB kit (Vector). The sections were counterstained with Haematoxylin of Harris.

RESULTS

Generation of K14-Cre transgenic mice expressing the Cre recombinase efficiently in the epidermis

To create somatic mutations in the epidermis, we engineered

mice expressing a K14-Cre transgene in which the Cre recombinase is expressed under the control of the human keratin 14 (K14) promoter (Vassar et al., 1989), which is active at the body surface of the mouse embryo as early as 9.5 days postcoitum (dpc) and is strongly upregulated by 14.5 dpc (Byrne et al., 1994; Vasioukhin et al., 1999). In postnatal mice, its activity is essentially restricted to the dividing basal layer keratinocytes of the epidermis, the outer root sheath (ORS) of hair follicles, and some other stratified squamous epithelia, e.g. oral and tongue epithelia (Wang et al., 1997). Three transgenic founder animals were identified by PCR and Southern blot analysis of tail DNA. All founders were fertile and yielded lines of transgenic mice that were bred with floxed ROSA26 Cre reporter transgenic mice (R26R in Soriano, 1999; called thereafter $ROSA^{fl/+}$) to yield $K14\text{-}Cre^{(tg/0)}/ROSA^{fl/+}$ double transgenic mice, in which translation of the β-galactosidase of the broadly active Cre reporter transgene occurs only upon Cre-mediated DNA excision. X-Gal staining was performed on newborns of all three double transgenic lines. β-galactosidase activity was detected in epidermis and hair buds (Fig. 1A,B, and data not shown). Semi-thin section analysis showed that it was uniformly distributed in the epidermis of one of the transgenic line (Fig. 1C,D), and could also be detected in tongue and salivary gland epithelial cells, but not in other tissues (data not shown). These results were correlated with Cre RNA in situ hybridisation analysis which showed the presence of Cre transcripts in epidermis, hair follicles, tongue and salivary glands (data not shown). Homogenous X-Gal staining was also seen in 15.5 dpc foetal epidermis (data not shown). Persistent homogenous X-Gal staining was observed throughout the epidermis and in hair follicles of adults of this double transgenic line (Fig. 1E,F), confirming the efficiency of Cre-mediated recombination. In contrast, X-Gal staining was patchy in the newborn and adult epidermis of the other double transgenic lines (data not shown). The transgenic line expressing Cre recombinase efficiently in the epidermis was named K14-Cre and used to selectively ablate RXRα.

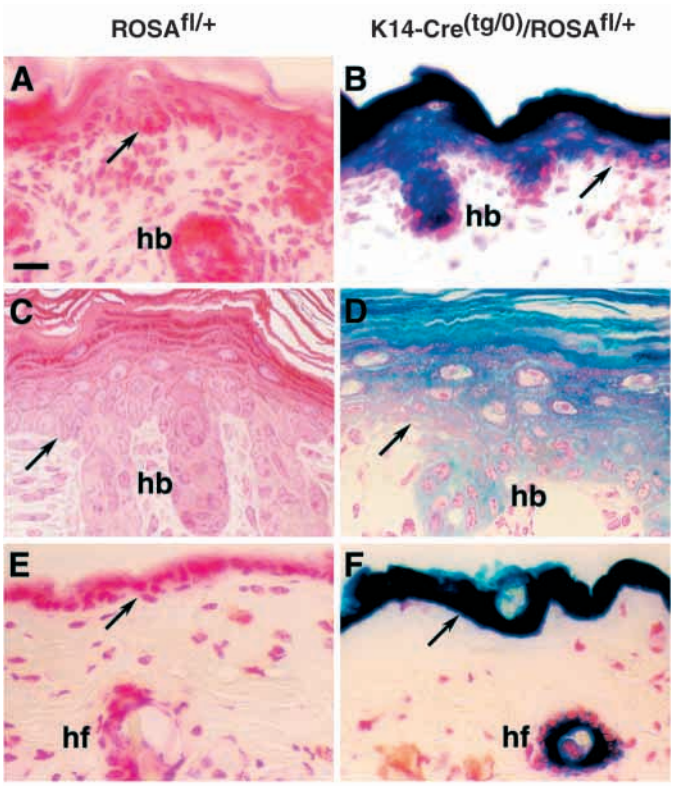

Fig. 1. Characterisation of Cre recombinase activity in skin of the K14-Cre transgenic line. X-Gal staining of skin sections taken from the back region of newborn (A-D) and 12-week-old mice (E-F). (A,C,E) Heterozygote ROSA Cre-reporter transgenic $ROSA^{fl/+}$; (B,D,F) double transgenic $K14\text{-}Cre^{(tg/0)}/ROSA^{fl/+}$. (A,B,E,F) 10 μm sections; (C,D) 2 μm sections. Sections were counterstained with safranin. Arrows point to the dermal/epidermal junction. hb, hair bud; hf, hair follicle. Scale bar: 16 μm for A,B,E,F; 12 μm for C,D.

Generation of mice harbouring floxed RXRα alleles

To conditionally disrupt the gene for RXRα (Kastner et al., 1994), we constructed the targeting vector $pRXR\alpha^{L2}$ that encompasses exons 2 to 4 (E2-E4) and contains a loxP site in the intron located upstream of exon 4, while a tk-neo selection cassette followed by another loxP site is present in the downstream intron 4 (Fig. 2A). Thus, homologous recombination of a wild-type allele with $pRXR\alpha^{L2}$ should allow a Cre recombinase-mediated excision of exon 4, together with the selection cassette, resulting in deletion of sequences encoding amino acids 149 to 209, which encompass the two zinc-finger motifs of the DNA-binding domain (Leid et al., 1992; Mangelsdorf et al., 1992; Kastner et al., 1994). Floxed RXRα L2 alleles were obtained through homologous recombination in ES cells (Fig. 2A, and data not shown; Materials and Methods). Chimeric males derived from two mutant ES clones transmitted the floxed allele through their germline (data not shown). Mice carrying one or two RXRα L2 alleles were indistinguishable from wild-type littermates (see below, and data not shown).

To verify that the floxed DNA segment of the RXRα L2 allele could be excised, $RXR\alpha^{L2/+}$ mice were crossed with CMV-Cre transgenic mice that express Cre recombinase in germ cells (Dupé et al., 1997). Southern blot analysis of double transgenic tail DNA showed that the floxed DNA segment was excised, thus resulting in an L– allele (Fig. 2A, data not shown). To compare this allele with the previously described RXRα null allele in which exon 4 is replaced by the neomycin resistance gene (RXRα (–) allele; Kastner et al., 1994; see also Fig. 2A), $RXR\alpha^{L-/+}$ and $RXR\alpha^{-/+}$ mice were bred. No 46 kDa protein corresponding to the expected product of the L– allele could be detected by western blot analysis performed on proteins extracted from 13.5 dpc $RXR\alpha^{L-/+}$ or $RXR\alpha^{L-/-}$ foetuses (data not shown), in agreement with our previous results showing that the RXRα (–) allele did not produce any truncated RXRα protein (Kastner et al., 1994). Furthermore, $RXR\alpha^{L-/-}$ and $RXR\alpha^{L-/L-}$ foetuses died between 12.5 and 16.5 dpc, and at 13.5 dpc, all of them exhibited ocular malformations, were often oedemic and had a whiter appearance, owing to poor vascular irrigation, all of which are characteristic features of $RXR\alpha^{-/-}$ embryos. However, $RXR\alpha^{L-/+}$ foetuses had a normal phenotype (data not shown; see Kastner et al., 1994). Thus, Cre-mediated recombination of the conditional RXRα L2 allele produces a RXRα null allele.

K14-Cre-mediated RXRα disruption in mouse epidermis

To selectively disrupt the gene for RXRα that is expressed in

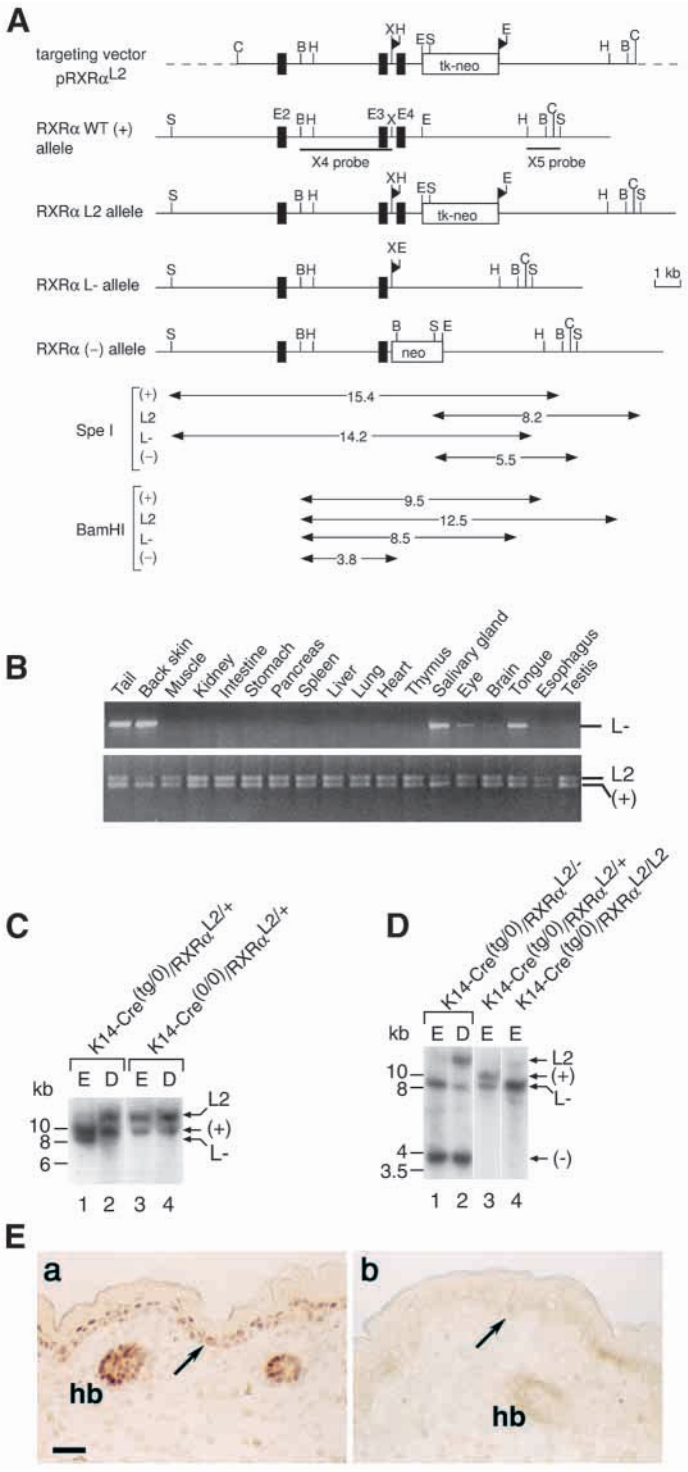

Fig. 2. Conditional mutagenesis of RXRα. (A) The pRXRα^{L2} targeting vector, the RXRα wild-type (+) genomic locus, the floxed RXRα L2 allele, the RXRα L– allele obtained after Cre-mediated excision of exon 4 and the RXRα (–) allele (Kastner et al., 1994). Black boxes correspond to exons. Restriction enzyme sites and the location of X4 and X5 probes are indicated. The numbers in the lower part of the diagram are in kilobases (kb). B, *Bam*HI; C, *Cla*I; E, *Eco*RI; H, *Hin*dIII; S, *Spe*I; X, *Xba*I. The broken line corresponds to backbone vector sequences. Arrowheads represent loxP sites. (B) Analysis of tissue-specificity of K14-Cre-mediated RXRα inactivation. (+), L2 and L– alleles were identified by PCR on DNA extracted from organs of 4-week-old K14-Cre$^{(tg/0)}$/RXRα$^{L2/+}$ mice. (C,D) Efficiency of K14-Cre-mediated RXRα recombination in 18.5 dpc (C) and adult (12-week-old) (D) skin. (+), L2, L– and (–) RXRα alleles were identified by Southern blot on DNA extracted from epidermis 'E' or dermis 'D' isolated from tail of animals with the indicated genotypes. Genomic DNA was digested with *Bam*HI and hybridised with X4 probe. (E) Immunohistochemical detection of RXRα on newborn skin sections from a K14-Cre$^{(0/0)}$/RXRα$^{L2/+}$ control (a) and K14-Cre$^{(tg/0)}$/RXRα$^{L2/–}$ mutant (b) mouse. Arrows point to the dermal/epidermal junction. hb, hair bud. Scale bar: 33 μm.

the epidermal keratinocyte and hair follicle ORS (see Fig. 2Ea, and data not shown), mice harbouring two floxed RXRα L2 alleles (RXRα$^{L2/L2}$) were bred with hemizygous K14-Cre$^{(tg/0)}$ mice. The specificity of exon 4 deletion was analysed by PCR on DNA extracted from various organs of 4-week-old K14-Cre$^{(tg/0)}$/RXRα$^{L2/+}$ mice. This deletion was readily detected in tail and back skin, as well as in tongue and salivary gland, but not in other tissues or at a much lower level (i.e. eye and brain; Fig. 2B).

The efficiency of exon 4 deletion in the foetal and adult epidermis was quantified by Southern blot, after separation of the epidermis from the dermis. In the epidermis of 18.5 dpc K14-Cre$^{(tg/0)}$/RXRα$^{L2/+}$ foetuses, the L–, but not the L2, allele was detected, whereas no L– allele was found in the dermis (Fig. 2C, lanes 1 and 2). As expected, no L– allele was found in either the epidermis or dermis of K14-Cre$^{(0/0)}$/RXRα$^{L2/+}$ mice (Fig. 2C, lanes 3 and 4). Furthermore, no RXRα protein was revealed by immunohistochemistry in K14-Cre$^{(tg/0)}$/RXRα$^{L2/–}$ newborn skin (Fig. 2E, compare panel a with panel b). Thus, Cre efficiently excised exon 4 of the floxed RXRα L2 allele in the developing epidermis. In adult (12-week-old) K14-Cre$^{(tg/0)}$/RXRα$^{L2/–}$ mice, the L2 allele was also efficiently recombined in the epidermis (Fig. 2D, lane 1), whereas trace amounts of L– DNA found in the dermis (Fig. 2D, lane 2) probably reflected a keratinocyte contamination that occurred during separation of epidermis from dermis (see Vasioukhin et al., 1999). Efficient RXRα mutation was also achieved in K14-Cre$^{(tg/0)}$/RXRα$^{L2/L2}$ mice that carry two L2 alleles (Fig. 2D, lane 4, and data not shown). As expected, no RXRα protein could be detected by immunohistochemistry in dorsal and ventral mutant epidermis and hair follicle (data not shown). Thus, the K14-Cre transgene efficiently and selectively disrupts floxed RXRα alleles in interfollicular epidermis and hair follicles.

K14-Cre-mediated RXRα disruption results in delayed postnatal hair follicle growth and epidermal maturation

To produce K14-Cre$^{(tg/0)}$/RXRα$^{L2/–}$ and K14-Cre$^{(tg/0)}$/RXRα$^{L2/L2}$ mutant mice in which RXRα was selectively disrupted in the epidermis, K14-Cre$^{(0/0)}$/RXRα$^{L2/L2}$ mice were bred to K14-Cre$^{(tg/0)}$/RXRα$^{+/–}$ and K14-Cre$^{(tg/0)}$/RXRα$^{L2/+}$ mice, respectively. Littermates (K14-Cre$^{(tg/0)}$/RXRα$^{L2/+}$, K14-Cre$^{(0/0)}$/RXRα$^{L2/–}$, K14-Cre$^{(0/0)}$/RXRα$^{L2/+}$ and K14-Cre$^{(0/0)}$/RXRα$^{L2/L2}$) were used as control animals. K14-Cre$^{(tg/0)}$/RXRα$^{L2/–}$ and K14-Cre$^{(tg/0)}$/RXRα$^{L2/L2}$ male and female mutant mice were born at Mendelian ratio and had the same external aspect as control animals, except that mutant skin was slightly shinier during the first day after birth (data not shown).

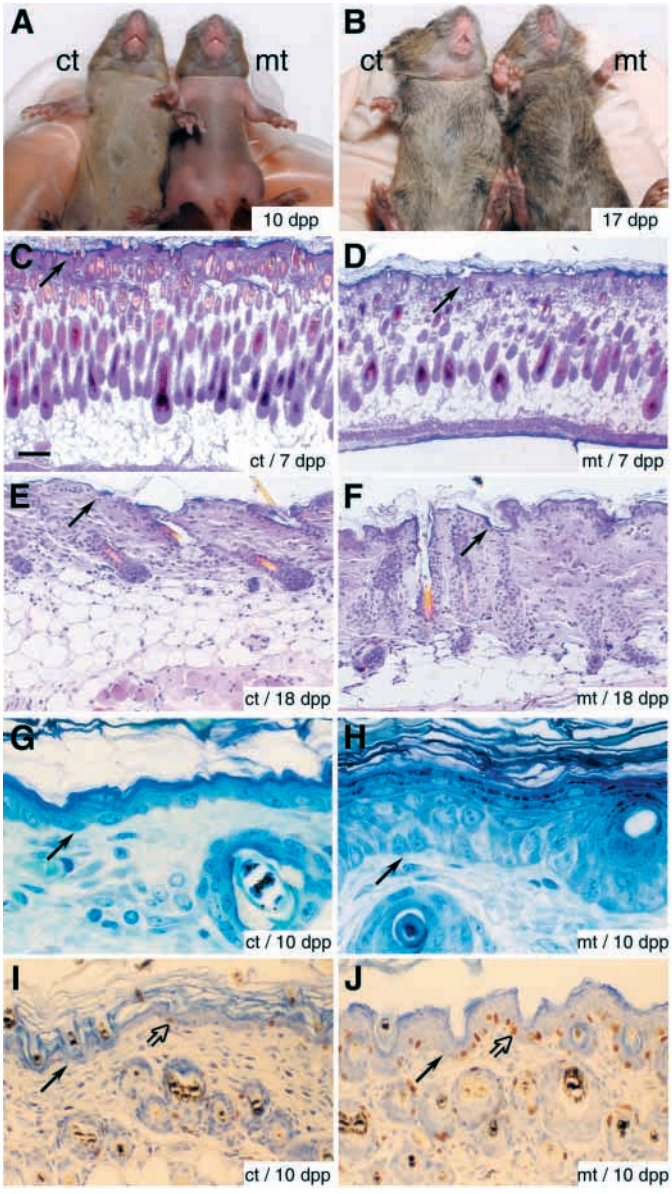

Fig. 3. Cre-mediated epidermal-selective inactivation of RXRα results in delayed post-natal skin maturation. Ventral view of 10 dpp (A) and 17 dpp (B) control (ct, K14-Cre$^{(tg/0)}$/RXRα$^{L2/+}$) and mutant (mt, K14-Cre$^{(tg/0)}$/RXRα$^{L2/L2}$) mice. (C-F) Haematoxylin and Eosin stained 5 μm paraffin sections of back skin from 7 dpp control (C) and mutant (D) mice, and from 18 dpp control (E) and mutant (F) mice. (G,H) Toluidine blue-stained 2 μm semi-thin section of back skin from 10 dpp control (G) and mutant (H) animals. (I,J) Epidermal proliferation in the skin of 10 dpp control (I) and mutant (J) mice, as determined by BrdU labelling experiments. Filled and open arrows point to the dermal/epidermal junction and to one of the BrdU-positive cells, respectively. Scale bar: 196 μm for C,D; 66 μm for E,F; 12 μm for G,H; 33 μm for I,J.

Interestingly, no difference in skin barrier acquisition between 17.5 dpc and birth was found when mutant and control mice were tested using a whole mount permeability assay (Hardman et al., 1998) (data not shown). However, the 'appearance' of hairs was delayed by 4-5 days in mutant mice, while they were visible by day 7 post-partum (dpp) in control littermates. In addition, 10 days after birth, the skin of mutant animals was more scaly over the entire surface of the body (Fig. 3A, and data not shown). These differences disappeared with time, and around 17 dpp, mutant and control mice had similar furs (Fig. 3B, and data not shown).

The mutant skin phenotype was further investigated at the histological level. No difference was observed between mutant and control skin of 18.5 dpc foetuses, newborn and 4-day-old mice (data not shown). In all cases, the epidermis was composed of the basal layer and more than four suprabasal layers, and hair follicles were similarly developed. At 7 dpp, the hair follicles of control skin were in anagen growth phase, characterised by the extension of follicles into thickened hypodermis, melanogenesis and presence of hair shafts (Fig. 3C). In contrast, follicular growth was delayed in mutant mice. Indeed, at 7 dpp the hypodermis was thinner, melanin synthesis was reduced and almost no hair shafts were observed (Fig. 3D), whereas in 9 dpp mutant mice, hair follicles were similarly developed as in 7 dpp control mice (data not shown). Furthermore, although at 18 dpp most, if not all, hair follicles were in telogen in control mice, only ~40% were in this stage in mutant mice, most of the others being in late catagen (Fig. 3E,F, and data not shown). At 20 dpp, almost all hair follicles were in telogen in both mutant and control mice (data not shown).

As previously described (Sundberg et al., 1996, and Refs therein), control mouse epidermis thickness decreased after birth as the hair coat develops, to reach 1-2 layers of suprabasal cells by 10 dpp (Fig. 3G). In contrast, more than four viable suprabasal layers were present in 10 dpp mutant mice (Fig. 3H). The stratum corneum of mutant epidermis was also thicker, in keeping with the more scaly appearance of mutant skin. These differences were observed in both dorsal and ventral mutant skin (data not shown). At this stage, the number of BrdU-positive keratinocytes was six- to sevenfold higher in basal layer cells of mutant (Fig. 3J) than in control (Fig. 3I) mice (16.0±1.2% and 2.5±0.2%, respectively), indicating a higher proliferation rate of mutant keratinocytes. In contrast, around 18 dpp, histological analysis revealed a similar number of BrdU-positive basal cell nuclei and epidermal suprabasal cell layers in mutant and control mice (data not shown), in accordance with the normal skin appearance.

The expression of keratins 5 (K5), 14 (K14), 10 (K10) and 6 (K6) is normally restricted to basal cells (K5 and K14), suprabasal cells (K10) and hair follicle (K6), and aberrant expression of K6 is known to be associated with pathological proliferation and differentiation (Porter et al., 1998). The keratin expression pattern of 10 dpp mutant skin was similar to that of 1 dpp to 5 dpp control skins, and no aberrant K6 expression was noticed in mutant skin (data not shown). By 18 dpp mutant and wild-type skins exhibited similar keratin expression pattern. Thus, postnatal skin maturation is delayed in mutant mice.

Alopecia and dermal cysts in mutant skin

Mutant mice developed a progressive alopecia. Hair loss started in ventral skin (near the legs), and extended to most regions of the ventral skin and some regions of the lower back skin (data not shown). In 12- to 16-week-old mutant mice, 80% of the ventral region was hairless and epidermal flaking was seen (Fig. 4A, and data not shown). In the dorsal skin, hair loss

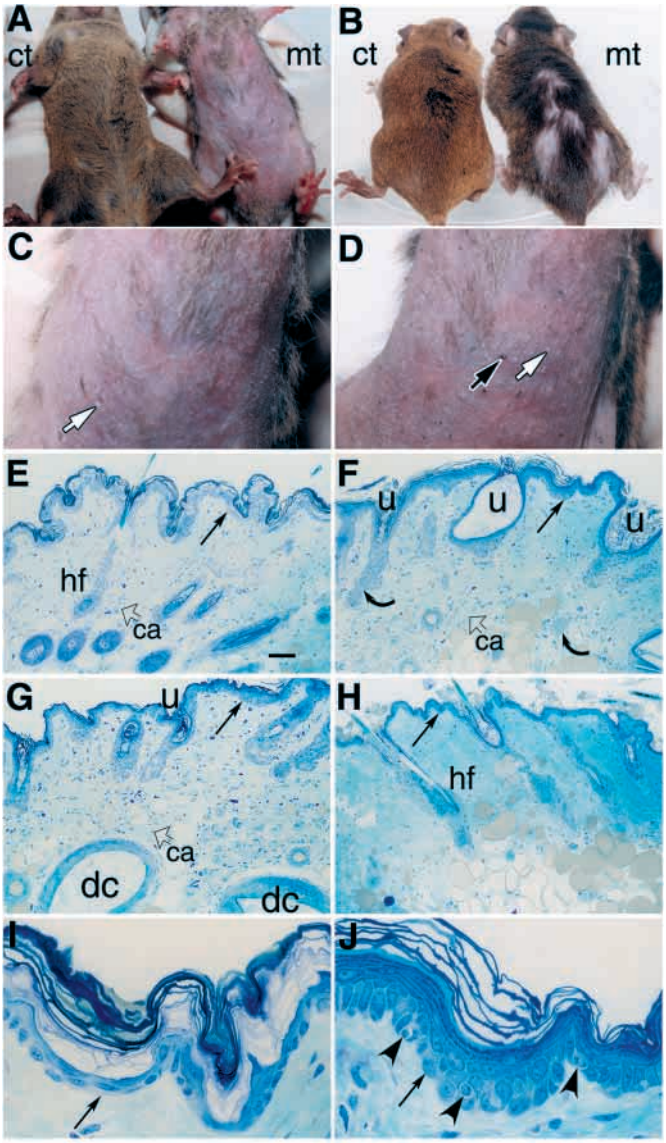

Fig. 4. Appearance of epidermal RXRα mutant mice and histological analysis of mutant skin. Ventral (A) and dorsal (B) view of 16-week-old control (ct, K14-Cre$^{(tg/0)}$/RXRα$^{L2/+}$) and mutant (mt, K14-Cre$^{(tg/0)}$/RXRα$^{L2/-}$) female mice. (C) Higher magnification view of mutant ventral skin shown in A. (D) Ventral view of the same mutant 18 weeks after birth. The white and the black arrows point to a cyst and a black 'dot' (see text), respectively. (E-J) Histological analysis of Toluidine Blue-stained 2 μm semi-thin sections. (E) Ventral skin of a 12-week-old control mouse. (F,G) Phenotypically abnormal ventral skin of a 12-week-old mutant. (H) Unaffected dorsal skin from a 12-week-old mutant mouse. dc, dermal cyst; hf, hair follicle; u, utriculus. Curved arrows in F point to the segregation of the distal from the proximal part of the hair follicle. Open arrows point to capillaries (ca). (I,J) Sections of control (I) and mutant (J) ventral epidermis at a higher magnification. Arrowheads point to Langerhans cells; arrows point to the dermal/epidermal junction. Scale bar: 60 μm for E-H; 12 μm for I,J.

was generally more patchy. Hair density was reduced in some regions of the back at the age of 4-5 weeks, and by the age of 12-16 weeks, 30-40% of the back was hairless (Fig. 4B, and data not shown). Hair loss was also observed around the eye (data not shown). In hairy regions, hairs were usually sparse and not uniformly oriented (data not shown). In black-coat mutant mice, hair colour became lighter and some grey/white-coloured hair was seen. This alopecia was less penetrant in approximately 20% of mutant males.

Many cysts were visible under the skin surface of hairless regions in all 13- to 15-week-old mutant females (Fig. 4C, and data not shown). With increasing age, the cysts became larger, and spread all over the body. In the mutant males that exhibited a less marked alopecia, cysts formed later and their number and size were reduced. In addition, black dots appeared in hairless ventral and dorsal skin of 13- to 15-week-old mutants. Their number increased with the age, and by 18 weeks they could be seen throughout the ventral skin and in part of the dorsal skin (Fig. 4D, and data not shown). The density of these black dots was higher in female than in male mutants. Finally, about 10% of mutant mice exhibited minor crusted skin lesions, mainly seen in dorsal hairless areas, on the chin and behind the ears (data not shown). These lesions did not result from fighting injuries, as the animals were housed separately.

Histological analysis of hairless ventral skin taken from 12-week-old mutants showed typical features of degenerated hair follicles. Many skin surface-connected ampuliform structures, that exhibited a dilatation of the piliary canal, a lack of hair shaft and were filled with horny cells (i.e. 'utriculi'; see Sundberg and King, 1996; Panteleyev et al., 1998) were observed in mutant skin (compare Fig. 4E control with Fig. 4F mutant). Another characteristic feature was the presence of closed, round dermal cysts that were embedded in the reticular dermis and not connected to the skin's surface (Fig. 4G). Segregation of the distal from the proximal part of the hair follicle was observed, resulting in the presence of cell clusters in the dermis (Fig. 4F). In ventral and dorsal regions exhibiting partial or no hair loss, some hair follicles were disorganised, while others still contained hair shafts (Fig. 4H, and data not shown). An increase in the number of epidermal cell layers was also observed in the affected regions (compare Fig. 4E and Fig. 4I control with Fig. 4F and Fig. 4J mutant). In regions with partial hair loss, this hyperplasia was mainly seen in areas adjacent to disorganised hair follicles (Fig. 4F,G) whereas, in the unaffected hairy regions, the epidermis consisted of 1-2 suprabasal cell layers (Fig. 4H and data not shown) as in control mice. Increased dermal cellularity was often observed underneath the hyperplastic epidermis, and many capillaries appeared dilated in mutant dermis, thus suggesting an inflammatory reaction (Fig. 4F,G, and see below).

The ultrastructure of mutant skin was also examined. The epidermis from control mice consisted of 1-2 suprabasal layers, with tightly apposed basal cells (Fig. 5A). In contrast, in mutants, the thickened epidermis was composed of more than four cell layers. In many (e.g. Fig. 5B), but not all (e.g. Fig. 5C), regions, gaps were observed between basal cells which appeared elongated (Fig. 5B). Interestingly, the number of Langerhans cells (Lc; dendritic cells containing cytoplasmic Birbeck's granules) (Katz et al., 1979), that are normally located in suprabasal layers of wild-type and littermate control skin (representing 3-8% of mammalian epidermal cells), was higher in mutant epidermis in which they were present in both suprabasal and basal cell layers (Fig. 5C; see also Fig. 4J, cells

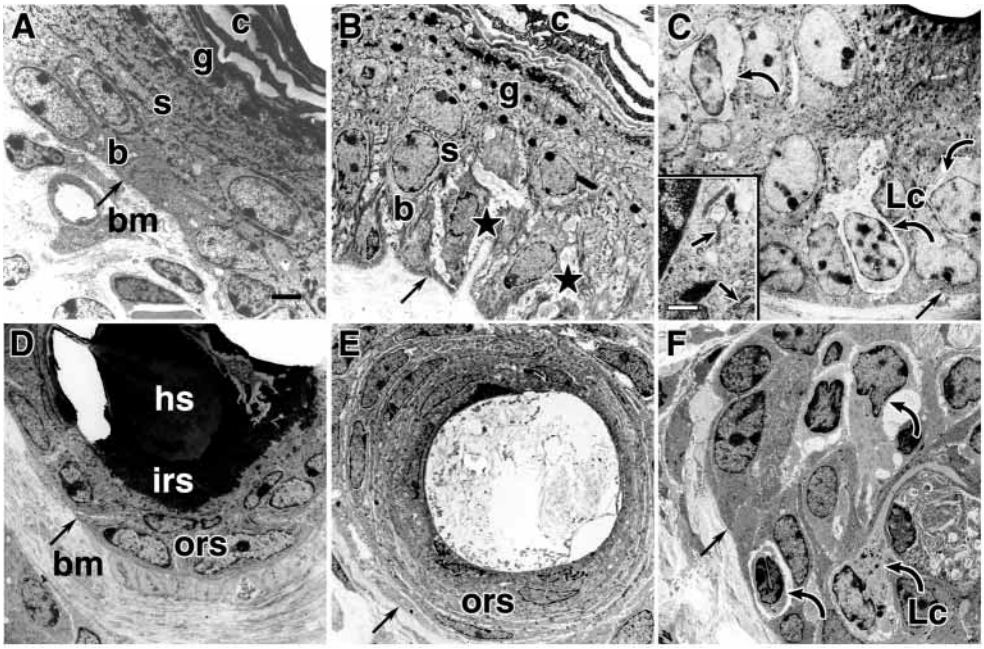

Fig. 5. Ultrastructure of epidermis and hair follicle of 12-week-old mouse mutant skin. (A) control (K14-Cre$^{(tg/0)}$/RXRα$^{L2/+}$) epidermis. (B,C) Mutant (K14-Cre$^{(tg/0)}$/RXRα$^{L2/-}$) epidermis. The gaps seen in B between basal cells are indicated by a star. b, basal layer; c, cornified layer; g, granular layer; s, spinous layer. (C) Another region of mutant epidermis in which gaps between basal cells are not seen. Curved arrows point to Langerhans cells (Lc) with characteristic cytoplasmic Birbeck's granules (C, insert in left bottom, small arrows). (D) Section through a control hair follicle. The outer root sheath (ors), the inner root sheath (irs) and the hair shaft (hs) are indicated. (E) Mutant utriculus. (F) Mutant dermal cyst exhibiting a multilayer keratinised epithelium wall. Curved arrows, Lc; arrows, basement membrane (bm). Scale bar: 2.5 μm for A-F; 0.25 μm for the inset.

with a pale cytoplasm). The ORS of the mutant utriculi consisted of four to six cell layers instead of one to two layers for normal control hair follicles, and intercellular gaps were also observed (compare Fig. 5D control with Fig. 5E mutant).

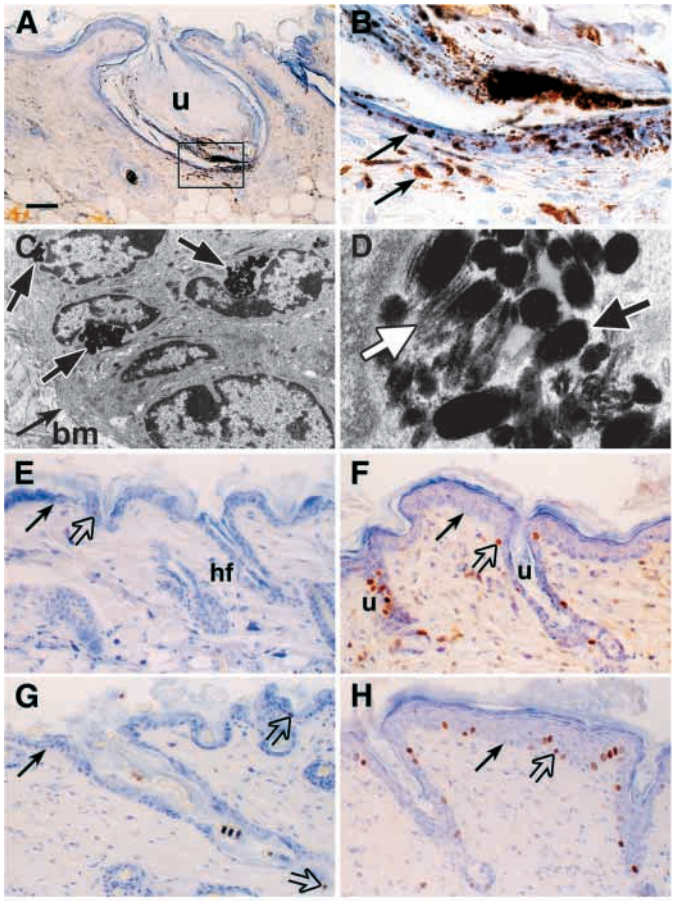

Dermal cysts were filled with cornified debris and sebum, and their wall consisted of a multilayer keratinised epithelium containing a number of Langerhans cells (Fig. 5F).

Skin sections also revealed an aggregation of melanosomes in the ORS of utriculi, and a mixture of melanin with horny cells inside utriculi (Fig. 6A,B). This is in contrast with the normal distribution of melanosomes that, in wild-type skin, are known to be present in melanocytes and surrounding keratinocytes of the hair bulb matrix to form melanised hair, but not in ORS keratinocytes (data not shown; for a review, see Hirobe, 1995). Note that some melanosomes were also found in adjacent dermis (Fig. 6A,B). Electron microscopic analysis showed the presence of compound melanosomes in the cytoplasm of ORS keratinocytes of mutant, but not of littermate control mice (Fig. 6C, and data not shown). Distinct stages of melanosome development (Ghadially, 1997) could be seen, including mature melanin granules (stage IV melanosome), and an earlier stage (stage III) that showed

Fig. 6. Analysis of melanosomes and keratinocyte proliferation in mutant skin. (A) 7 μm paraffin sections of skin from a 18-week-old K14-Cre$^{(tg/0)}$/RXRα$^{L2/-}$ mutant mouse, stained with Haematoxylin of Harris. (B) Higher magnification of the boxed region in A. The aggregation of melanosomes in the outer root sheath of one utriculus (u) and in the dermis are indicated by arrows. (C,D) Electron microscopic analysis. The compound melanosomes within keratinocytes in C are indicated by large arrows. The small arrow points to the basement membrane (bm). (D) Different stages of melanosomes; white arrow, stage III; black arrow, stage IV. (E-H) Analysis of keratinocyte proliferation as determined by BrdU-labelling experiments. (E,F) Samples from 7-week-old control and mutant ventral skin, respectively. (G,H) Samples from 11-week-old control and mutant ventral skin, respectively. Open arrows point to all visible BrdU-labelled cells in E,G, and one of the positive cells in F,H. Black arrows point to dermal/epidermal junctions. hf, hair follicle; u, utriculi. Scale bar: 60 μm for A; 12 μm for B; 1 μm for C; 0.1 μm for D; 33 μm for E-H.

melanin deposition while the internal structure was still visible (Fig. 6D).

Impaired anagen initiation of hair follicle cycle in mutant mice

To analyse the role of RXRα in hair cycle regulation, 20 dpp mice were subjected to depilation of dorsal hair to induce a synchronised anagen wave. As expected, in control mice progressive skin pigmentation was observed 5 to 6 days post-depilation (dpd), and hair appeared at 10 dpd (Fig. 7A, left; and data not shown). In contrast, mutant mice did not show any induction of skin pigmentation at 6 dpd, and at 10 dpd patchy skin pigmentation was observed only in the anterior region (Fig. 7A, right; and data not shown). At 24 dpd, only patchy fur had developed in mutant mice, whereas fur of control mice was similar to that non-depilated mice (Fig. 7B). Moreover, in black-coated mutants, 80% of the new hair was grey or white (data not shown). Histological analysis of control mouse skin showed anagen induction at 6 dpd and the presence of mature hair follicles at 10 dpd (Fig. 7C,E). In contrast, no anagen hair follicles were observed in 6 dpd mutant skin, and at 10 dpd, most of the hair follicles were arrested in telogen (Fig. 7D,F). A number of hair follicles of mutant mice were still in telogen at 24 dpd, while the others were mostly in anagen, but were markedly enlarged and/or misoriented (Fig. 7H, and data not shown). In contrast, at this time, hair follicles of control mice had already reached the catagen or telogen stage (Fig. 7G). Thus, these data demonstrate that RXRα plays a key role in initiation of anagen during hair follicle cycling.

Alteration of cell proliferation and terminal differentiation in mutant epidermis

BrdU incorporation was used to estimate the rate of cell proliferation. In 7-week-old mutant mice, a marked increase in the number of BrdU-positive nuclei was noticed in phenotypically abnormal hair follicles, when compared with control skin of the same age. An increase in the number of BrdU-positive cells was also detected in interfollicular mutant epidermis (Fig. 6E,F, and data not shown). In 11-week-old mutant mice, the number of BrdU-positive nuclei was markedly increased, notably in utriculi, as well as in interfollicular basal cells close to utriculi (compare Fig. 6G with Fig. 6H). The epithelium of dermal cysts also showed a high incorporation of BrdU (data not shown). Determination of the percentage of BrdU-labelled basal cells in the mutant mice (more than 3000 basal cells were counted in different areas of skin sections) revealed that 9.4±0.7% of basal cells were BrdU-positive in mutant epidermis, versus 1.0±0.1% in control epidermis. This keratinocyte proliferation was confirmed by immunostaining for Ki-67, a nuclear protein expressed by proliferating cells (Schlüter et al., 1993). Note that no increase of BrdU labelling was observed in unaffected regions of mutant skin (data not shown). Collectively, these results indicate that RXRα ablation in the epidermis results in increased basal and utricular keratinocyte proliferation.

Immunohistochemical analysis of epidermal differentiation was performed on skin biopsies from 16-week-old animals using several markers (Fig. 8). In wild-type adult mouse, K14 and K5 are expressed in the basal cell layer, while K10 expression is restricted to suprabasal cells, filaggrin to the granular layer, and K6 is expressed in hair follicles, but not in

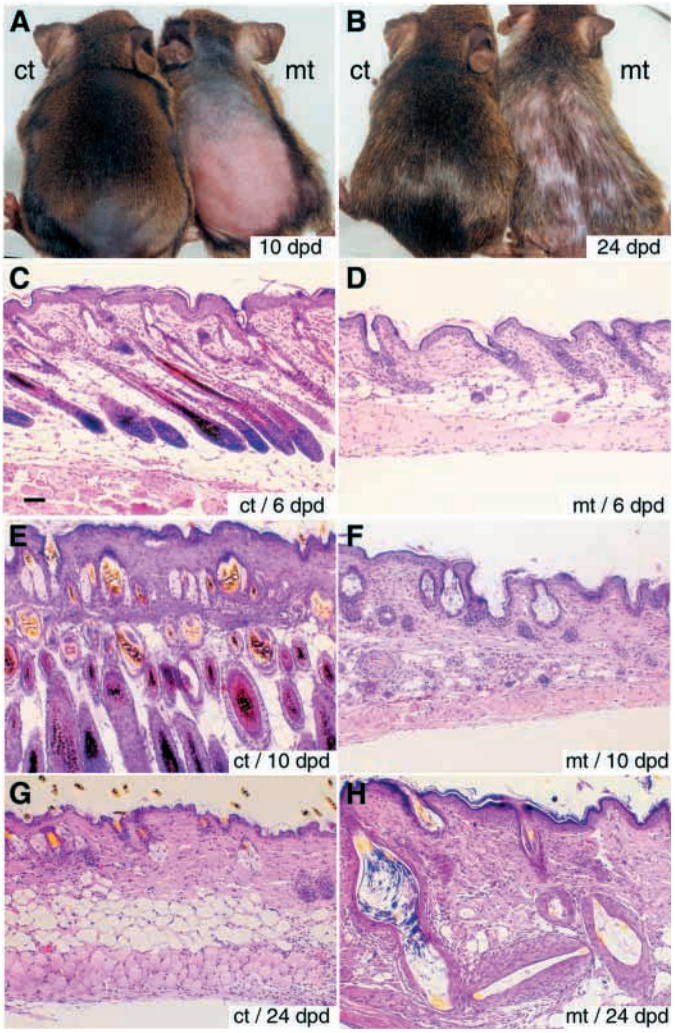

Fig. 7. Impaired anagen initiation after hair depilation of RXRα mutant mice. Dorsal view of a control (ct, K14-Cre$^{(tg/0)}$/RXRα$^{L2/+}$) and a mutant (mt, K14-Cre$^{(tg/0)}$/RXRα$^{L2/-}$) female mouse at 10 (A) and 24 (B) dpd (days post depilation). (C-H) Haematoxylin and Eosin stained 5 μm paraffin sections of depilated control and mutant skin at 6 dpd (C,D), 10 dpd (E,F) and 24 dpd (G,H). Scale bar: 66 μm for C-H.

interfollicular epidermis. In control skin and 'phenotypically normal' regions of mutant skin, K14 and K5 were expressed as expected in the epidermis basal cell layer (Fig. 8A,C, and data not shown). In contrast, while K14 was mainly expressed in the basal layer of mutant skin with some extension into the suprabasal layer (Fig. 8B), K5 was expressed in almost all cell layers (Fig. 8D). K10 and filaggrin expression was thickened in mutant skin, but restricted to hyperplastic suprabasal and granular layers, respectively (compare Fig. 8E,G with Fig. 8F,H). However, K6 was aberrantly expressed throughout all layers of hyperproliferative interfollicular epidermis of mutant skin (compare Fig. 8I with Fig. 8J), demonstrating that terminal differentiation is altered in epidermal keratinocytes lacking RXRα.

Presence of an inflammatory infiltrate in mutant skin

Inflammation in mutant skin was suggested by an increase in dermal cellularity underneath the hyperplastic epidermis, the

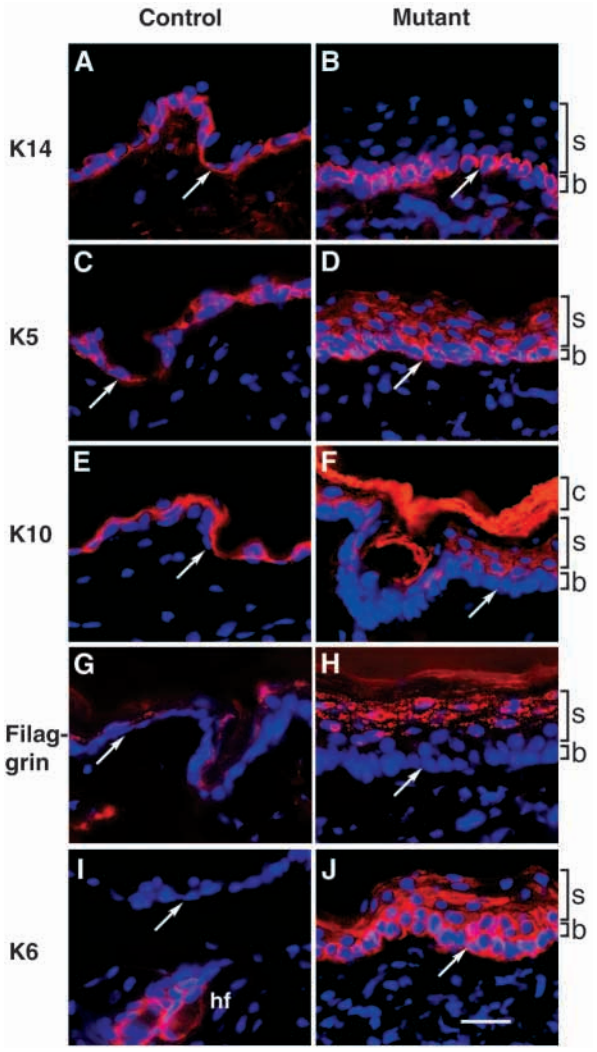

Fig. 8. Altered terminal differentiation in mutant epidermis. (A-J) Skin sections from 16-week-old control (K14-Cre$^{(tg/0)}$/RXRα$^{L2/+}$) (left) and mutant (K14-Cre$^{(tg/0)}$/RXRα$^{L2/-}$) (right) mice were stained with antibodies against keratin 14 (K14; A,B), keratin 5 (K5; C,D), keratin 10 (K10; E,F), filaggrin (G,H) and keratin 6 (K6; I,J). The red corresponds to the staining of the antibodies, and the blue corresponds to the DAPI DNA staining. Arrows point to the dermal/epidermal junction. b, basal layer; c, cornified layer; hf, hair follicle; s, suprabasal layer. Scale bar: 25 μm.

presence of dilated dermal capillaries (see Fig. 4F,G and compare Fig. 9A with Fig. 9E, in which endothelial intercellular junctions are labelled with anti-CD31 antibodies (Charpin et al., 1995)), and a marked increase in epidermal Langerhans cells (Figs 4J, 5C). To investigate the nature of the inflammatory infiltrate, sections of 16-week-old control and mutant ventral skin were immunoreacted with antibodies to the T lymphocyte markers CD3, CD4 and CD8. Control skin contained scattered CD3-positive cells (most probably γδ-T cells; Asarnow et al., 1988) in the epidermis (Fig. 9B), few CD4-positive cells (most probably helper T cells) in the dermis (Fig. 9C) and no CD8-positive cells (cytotoxic T cells; data not shown). In mutant skin, the number of CD3-positive cells was increased in the epidermis and in the dermis (Fig. 9F). Numerous CD4-positive cells were present in mutant dermis, utriculi and dermal cysts, and few CD4-positive cells were detected in the epidermis (Fig. 9G, and data not shown). In contrast, no CD8-positive cells were detected in mutant epidermis and dermis (data not shown). Staining with anti-F4/80 (Austyn and Gordon, 1981) and anti-NLDC145 (Swiggard, 1995) antibodies indicated an increase of macrophages and dendritic cells, respectively, in mutant dermis (data not shown). An increase in mast cells was also seen in the dermis of mutant animals, as revealed by Giemsa staining and electron microscopy analysis (data not shown). Skin sections were also probed for ICAM1 (CD54), which is induced on the surface of keratinocytes by proinflammatory stimuli (for a review, see Springer, 1990; Carroll et al., 1995). While a weak expression of ICAM1 was seen in control skin, an intense ICAM1 staining was observed on all cell layers of mutant epidermis, as well as on cells of the dermis (Fig. 9D,H). Note that Gram and periodic acid-Schiff reagent staining did not reveal any sign of bacterial or fungal infection in mutant skin that exhibited the above immune response, and no B lymphocytes could be detected using antibodies to B lymphocyte IgM and CD45R (data not shown).

To determine whether hair follicle degeneration accounts for this immune response, VDR-null mice, which exhibit an alopecia resembling that seen in the RXRα mutant mice described above (Li et al., 1997; Li et al., 1998; Li et al., 2000; Yoshizawa et al., 1997; Sakai and Demay, 2000), were analysed. Although the dermis of VDR null mutant exhibited a modest increase in CD4-positive lymphocytes and macrophages (Fig. 9K, and data not shown), no dermal capillaries enlargement was observed (Fig. 9I), and there was no change in the number of dendritic cells and mast cells in the dermis (data not shown). Similarly, CD3-positive and Langerhans cells were not increased in the epidermis, and ICAM1 expression was not induced at the surface of *Vdr*$^{-/-}$ epidermal keratinocytes (Fig. 9J,L), indicating the absence of proinflammatory stimuli. Thus, VDR-null mice develop a very limited skin inflammatory reaction, in agreement with previous observations (Sakai and Demay, 2000; Li et al., 2000). Therefore, the immune response in RXRα mutant skin does not appear to be secondary to hair follicle defects.

DISCUSSION

RXRα ablation in keratinocytes does not affect foetal development of mouse skin, but delays its postnatal maturation

We have shown here that the skin of newborns, in which a somatic RXRα-null mutation has been generated in epidermal keratinocytes at early stages of their foetal differentiation, is apparently normal both morphologically (although somewhat shinier) and functionally (no obvious defects in barrier function). Thus, RXRα does not appear to be indispensable in keratinocytes for epidermis development. RXRβ is also expressed in newborn epidermis (M. L., P. C. and D. M., unpublished observations) and RXRβ null newborns do not exhibit any obvious skin defects (Kastner et al., 1996). We are presently introducing the RXRα-null keratinocyte-specific somatic mutation in RXRβ null mice to investigate the possibility that functional redundancy between RXRα and

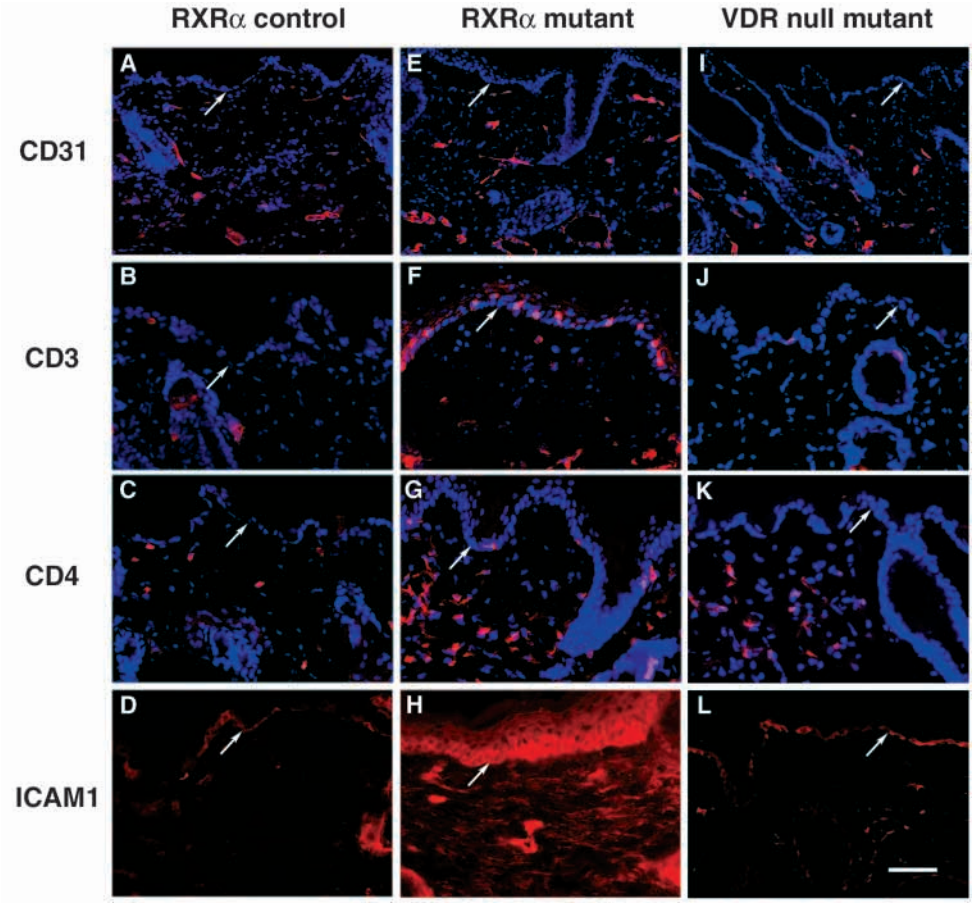

Fig. 9. Inflammation infiltrate in RXRα mutant skin and in VDR null mutant skin. (A-L) Skin sections from 16-week-old RXRα control (K14-Cre$^{(tg/0)}$/RXRα$^{L2/+}$) (left), RXRα mutant (K14-Cre$^{(tg/0)}$/RXRα$^{L2/-}$) (middle), and VDR null mutant (right) mice were stained with antibodies to CD31 (A,E,I), CD3 (B,F,J), CD4 (C,G,K) and ICAM1 (CD54; D,H,L). The red corresponds to the staining of the antibodies, and the blue to the DAPI DNA staining. Arrows point to the dermal/epidermal junction. Scale bar: 90 μm for A,E,I; 50 μm for B-D,F-H,J-L.

RXRβ could account for the dispensability of keratinocyte RXRα during epidermis development.

Although RXRα ablation in foetal epidermal keratinocytes has very little effect in newborns, our study reveals that the mutants exhibit a delay in postnatal hair follicle growth and epidermis maturation. As these mutants were not growth-retarded (data not shown), the retardation in epidermis thinning could be secondary to the delay in hair follicle growth.

Ligand deprivation and pharmacological studies in vivo, as well as on keratinocytes in culture, have suggested that retinoids are physiologically involved in epidermis development and keratinocyte differentiation (for Refs, see Fischer and Voorhees, 1996; Imakado et al., 1995; Xiao et al., 1999). RAR/RXR heterodimers are believed to mediate these actions (Kastner et al., 1995; Kastner et al., 1997; Mangelsdorf et al., 1995; Chambon, 1996; and Refs therein). However, knockout of either RARα (Lufkin et al., 1993) or RARγ (Lohnes et al., 1993) has no or little effect on epidermal cellularity and structure, which appear normal at adult stages. Interestingly, RARγ null newborns exhibit a shiny skin phenotype, similar to that of the present mutants, which dissipates within few days after birth (N. Ghyselinck, W. Krezel, N. M., Ph. Kastner and P. C., unpublished observations). Functional redundancy between RARα and RARγ could account for this lack of major skin alterations, but the epidermis of the few RARα/RARγ double null mutant foetuses that could be examined externally at 18.5 dpc did not appear severely affected (Lohnes et al., 1994). Interestingly, targeted overexpression of a dominant negative RXRα mutant in foetal suprabasal keratinocytes did not result in skin development abnormalities, although it significantly inhibited RA-induced basal cell hyperproliferation (Feng et al., 1997). In contrast, foetal overexpression of dominant negative RARα mutants in suprabasal (Imakado et al., 1995) or basal (Saitou et al., 1995) keratinocytes led to severe impairment of skin barrier function, together with either high neonatal lethality or dramatic suppression of epidermal development and lethality shortly after birth, respectively. However, another foetal overexpression of dominant negative RARα mutant in suprabasal keratinocytes had very little effect, as newborns exhibited the RARγ KO shiny phenotype only, and epidermal cellularity and structure appeared to be normal at adult stages, while RA-induced basal cell hyperproliferation was inhibited (Xiao et al., 1999).

These variable effects of dominant negative RAR mutants suggest, but by no means prove that RA is physiologically involved in epidermal development, as overexpression of dominant negative RAR mutants may artefactually lead to repression of genes that are not normally targeted by corepressor-associated unliganded RAR/RXR heterodimers (Chen and Evans, 1995) and/or interfere with functions of other RXR heterodimeric partners (see below) through sequestration of RXRs. Ablation of all three RARs in keratinocytes during foetal life is obviously necessary to elucidate whether RA is physiologically required for epidermal morphogenesis.

RXRα/VDR heterodimer involvement in hair-follicle cycling

Normal morphogenesis and cycling of hair follicles is

dependent on a series of mesenchymal-epithelial interactions (reviewed in Hardy, 1992; Sundberg et al., 1996; Oro and Scott, 1998; Paus and Cotsarelis, 1999; and Refs therein). Mice are born with no external evidence of hair. The first follicle growth phase that is initiated in utero persists until around 14 dpp (hair become apparent by 7 dpp), when the follicle enters the first catagen stage. Within 3 days, this involution stage is completed and after a short 3 day telogen resting phase, the second cycle starts. The intervals between the cycles, that are repeated throughout the life of the mouse, increase with age to become erratic with prolonged periods of telogen, while the cycle stage is predictable at specific anatomic sites during the first two cycles (see Sundberg and King, 1996; Sundberg et al., 1996).

Even though primary hair growth is somewhat delayed in RXRα mutants, the first hair coat appears normal and no defects are observed in the hair follicle at the end of the first hair cycle. However, these mutants subsequently lose their hair to develop, by the age of 4 to 6 weeks, an alopecia, which is extensive by 10-12 weeks of age. Our results show that hair loss results from a requirement for RXRα at the anagen initiation stage of the hair cycle. The progression of alopecia might reflect a partial functional redundancy between RXRα and RXRβ, as recently suggested from the study of mice in which RXRα was ablated in the epidermis at the adult stage (Li et al., 2000). Such a redundancy might also account for the greater severity of alopecia in females than in males, which have higher levels of RXRβ in the skin (Li et al., 2000). It could also account for dorso-ventral differences in alopecia, as higher RXRβ levels are found in dorsal than ventral skin (M. L., P. C. and D. M., unpublished observations).

Mice bearing mutations at the hairless (*hr*) locus also exhibit a postnatal alopecia, following normal hair morphogenesis with the development of an apparently normal first hair coat up to 13-14 dpp (Panteleyev et al., 1988). Utriculi and dermal cysts that are similar to those of our RXRα-ablated mutants are also formed. However, hair loss in homozygous hairless mice is rapid and sharply demarcated, leading to an almost complete alopecia at the age of 3 weeks. Moreover, the main failure in hair follicles of *hr*/*hr* mice occurs during the first catagen stage (Panteleyev et al., 1998 and Refs therein), in contrast to RXRα mutants, and hairless RNA levels are normal in our RXRα-ablated mutants (M. L., P. C. and D. M., unpublished observations). Therefore, it appears unlikely that the hair follicle defects seen in our RXRα-ablated mutants could reflect an involvement of RXRα in control of expression of the *hr* gene.

The vitamin D3 receptor (VDR) is differentially expressed during distinct hair cycle stages in both the ORS and dermal papilla of mouse hair follicle (Reichrath et al., 1994). Most interestingly, VDR mutations in humans (Malloy et al., 1999) and *Vdr* gene knockouts in mice (Li et al., 1997; Li et al., 1998; Yoshizawa et al., 1997; Sakai and Demay, 2000) result in alopecia, which, in mice, resembles that exhibited by mice in which RXRα has been ablated in keratinocytes during skin morphogenesis (the present study) or in keratinocytes of adult animals (Li et al., 2000). As in RXRα mutant mice, the onset of alopecia appears to be secondary to a defect occurring at the anagen phase of the second hair cycle (Sakai and Demay, 2000; M. L., H. C., X. W., N. M., C. G., P. C. and D. M., unpublished observations). It is noteworthy that VDR levels are not reduced in the skin of RXRα mutant mice, and that in contrast to these mutants, hair morphogenesis is normal in VDR null mutants (M. L., H. C., X. W., N. M., C. G., P. C. and D. M., unpublished observations; Sakai and Demay, 2000). Thus, heterodimers of RXR and VDR could play an important role in the initiation of the anagen during the hair follicle cycle, whereas other RXRα heterodimeric partners (see below) might be involved in postnatal hair follicle development.

The absence of alopecia in kindreds with vitamin D-dependent rickets type I (VDDRI) (due to 25(OH)D3 1α-hydroxylase mutations; Malloy et al., 1999), as well as in profound vitamin D deficiency, further suggest that VDR could function in a ligand-independent manner, within these heterodimers, perhaps by repressing the expression of target gene(s) (Yen et al., 1996). Alternatively, the activity of the heterodimer could be induced by ligand(s) that bind(s) the RXRα partner. Further keratinocyte-specific temporally controlled somatic mutations of RXRα and VDR, notably of their AF2 ligand-dependent activation functions, are required to elucidate the possible role of RXRα/VDR heterodimers in hair follicle homeostasis.

RXRα involvement in homeostasis of both keratinocyte proliferation/differentiation and skin immune system

We have shown here that RXRα ablation in basal keratinocytes results in hyperproliferation and abnormal differentiation of interfollicular epidermal keratinocytes in adult mice. The increased number of suprabasal layers is correlated with increased proliferation of mutant epidermal basal keratinocytes, whereas the perturbation of terminal differentiation is reflected by aberrant expression of keratins in the hyperproliferative epidermis, most notably of K6 that is normally confined to hair follicles. Most interestingly, these hyperproliferation/differentiation abnormalities in interfollicular epidermis have not been observed in VDR null mutants (Sakai and Demay, 2000; Li et al., 2000; M. L., N. M., C. G., P. C. and D. M., unpublished observations), even though the hair follicle defects are highly similar in these mutants and our RXRα mutants (see above). These observations therefore suggest that RXRα may exert functions in proliferation/differentiation of epidermal keratinocytes that are distinct from those mediated through RXRα/VDR heterodimers in hair-follicle cycling.

The inflammatory infiltrate present in the skin of adult animals, in which RXRα has been ablated in basal keratinocytes, does not appear to correspond to an immune response to foreign antigens, as there is no evidence for bacterial or fungal infection. It is much more likely that it is triggered by cytokines and chemokines released by the aberrantly differentiated keratinocytes. For instance, keratinocytes have been identified as targets of GM-CSF, and also shown to release this cytokine under pathological conditions and after wounding (Breuhahn et al., 2000; and Refs therein; see also Miranda and Granstein, 1998). Further studies are now required to characterise this immune response and identify the cytokines/chemokines released by RXRα-ablated keratinocytes. In any event this immune response does not appear to be secondary to hair follicle defects, as there is very little inflammatory reaction in VDR null mice. Thus RXRα ablation in epidermal keratinocytes results in an inflammatory reaction in which RXRα/VDR heterodimers are not crucially involved.

RXRs are known to heterodimerise in vitro and in cells in culture with a number of nuclear receptors including (in addition to VDR) RARs, TRs, PPARs, LXRs, FXR and several orphan receptors (Mangelsdorf et al., 1995; Chambon, 1996; Giguère, 1999). In a limited number of cases, genetic evidence has confirmed that such heterodimers act as signal transducers in the mouse (Kastner et al., 1997; Mascrez et al., 1998; Wendling et al., 1999; Wan et al., 2000). Ligand depletion and pharmacological studies have suggested that some of these NRs, which are present in the skin, could be crucial regulators in development and homeostasis of epidermis and hair follicle (Fisher and Voorhees, 1996; Yoshizawa et al., 1997; Li et al., 1997; Li et al., 1998; Kömüves et al., 1998; Hanley et al., 1997; Hanley et al., 1998; Hanley et al., 2000a; Hanley et al., 2000b; Peters et al., 2000; Billoni et al., 1997; Billoni et al., 2000a; Billoni et al., 2000b). However, individual disruption of a number of these receptors has not yet revealed their possible role in the skin, owing, in some cases, to the lethality of the mutation in utero or shortly after birth, and in other cases most probably because of functional redundancies. Further genetic studies aimed at disrupting in adult mice both partners of the various skin-expressed RXRα/NR heterodimers through spatio-temporally controlled somatic mutagenesis (Li et al., 2000) should reveal which RXRα partners, beside VDR, are involved in the abnormalities resulting from RXRα ablation in keratinocytes.

We are grateful to S. Werner for the human K14 promoter, to P. Soriano, S. Kato and Ph. Kastner for Rosa R26R, *Vdr*$^{-/-}$ and RXRα$^{+/-}$ mice; to B. Lane for K5, K10 and K14 antibodies; and to C. Rochette-Egly, Y. Lutz and M. Oulad-Abdelghani for biotin-conjugated 4RX3A2 antibody. We thank J. M. Bornert, S. Bronner, and N. Chartoire for technical assistance, as well as the staff of the animal facility. We also thank J. L. Vonesch for confocal microscopy, and S. Chen, M. Mark and P. Dollé for useful discussions. This work was supported by funds from the Centre National de la Recherche Scientifique, the Institut National de la Santé et de la Recherche Médicale, the Collège de France, the Hôpital Universitaire de Strasbourg, the Association pour la Recherche sur le Cancer, the Fondation pour la Recherche Médicale, the Human Frontier Science Program, the Ministère de l'Éducation Nationale de la Recherche et de la Technologie and the European Economic Community. M. L. was supported by fellowships from the Association pour la Recherche sur le Cancer and the Fondation pour la Recherche Médicale; H. C. by fellowships from the Centre National de la Recherche Scientifique and the Fondation pour la Recherche Médicale; and X. W. by fellowships from the Ministère de l'Education Nationale, de la Recherche et de la Technologie and from the Fondation pour la Recherche Médicale.

REFERENCES

Asarnow, D. M., Kuziel, W. A., Bonyhadi, M., Tigelaar, R. E., Tucker, P. W. and Allison, J. P. (1988). Limited diversity of gamma delta antigen receptor genes of Thy-1+ dendritic epidermal cells. *Cell* **55**, 837-847.

Austyn, J. M. and Gordon, S. (1981). F4/80 a monoclonal antibody directed specifically against the mouse macrophage. *Eur. J. Immunol*. **11**, 805.

Billoni, N., Gautier, B., Mahé, Y. F. and Bernard, B. A. (1997) Expression of retinoid nuclear receptor superfamily members in human hair follicles and its implication in hair growth. *Acta Derm. Venerol.* **77**, 350-355.

Billoni, N., Buan, B., Gautier, B., Gaillard, O., Mahé, Y. F. and Bernard, B. A. (2000a) Thyroid hormone receptor beta1 is expressed in the human hair follicle. *Br. J. Dermatol.* **142**, 645-652.

Billoni, N., Buan, B., Gautier, B., Collin, C., Gaillard, O., Mahé, Y. F. and Bernard, B. A. (2000b) Expression of peroxisome proliferator activated receptors (PPARs) in human hair follicles and PPARα involment in hair growth. *Acta Derm. Venerol.* **80**, 1-7.

Breuhahn, K., Mann, A., Müller, G., Wilhelmi, A., Schirmacher, P., Enk, A. and Blessing, M. (2000). Epidermal overexpression of granulocyte-macrophage colony-stimulating factor induces both keratinocyte proliferation and apoptosis. *Cell Growth Diff.* **11**, 111-121.

Brocard, J., Warot, X., Wendling, O., Messaddeq, N., Vonesch, J. L., Chambon, P. and Metzger, D. (1997). Spatio-temporally controlled site-specific somatic mutagenesis in the mouse. *Proc. Natl. Acad. Sci. USA* **94**, 14559-14563.

Byrne, C., Tainsky, M. and Fuchs, E. (1994). Programming gene expression in developing epidermis. *Development* **120**, 2369-2383.

Carroll, J. M., Romero, M. R. and Watt, F. M. (1995). Suprabasal integrin expression in the epidermis of transgenic mice results in developmental defects and a phenotype resembling psoriasis. *Cell* **83**, 957-968.

Chambon, P. (1996). A decade of molecular biology of retinoic acid receptors. *FASEB J*. **10**, 940-945.

Charpin, C., Devictor, B., Bergeret, D., Andrac, L., Boulat, J., Horschowski, N., Lavaut, M. N. and Piana, L. (1995). CD31 quantitative immunocytochemical assays in breast carcinomas. Correlation with current prognostic factors. *Am. J. Clin. Pathol.* **103**, 443-448.

Chen, J. D. and Evans, R. M. (1995). A transcriptional co-repressor that interacts with nuclear hormone receptors. *Nature* **377**, 454-457.

Clifford, J., Chiba, H., Sobieszczuk, D., Metzger, D. and Chambon, P. (1996). RXRalpha-null F9 embryonal carcinoma cells are resistant to the differentiation, anti-proliferative and apoptotic effects of retinoids. *EMBO J*. **15**, 4142-4155.

DuBrul, E. (1972). Fine structure of epidermal differentiation in the mouse. *J. Exp. Zool*. **181**, 145-158.

Dierich, A. and Dollé, P. (1997). Gene targeting in embryonic stem cells. In *Methods in Development Biology/Toxicology* (ed. S. Klug and R. Thiel), pp. 111-123. Oxford: Blackwell.

Dupé, V., Davenne, M., Brocard, J., Dollé, P., Mark, M., Dierich, A., Chambon, P. and Rijli, F. M. (1997). In vivo functional analysis of the Hoxa-1 3′ retinoic acid response element (3′RARE). *Development*. **124**, 399-410.

Elder, J. T., Astrom, A., Pettersson, U., Tavakkol, A., Christopher, E. M. G, Krust, A., Kastner, P., Chambon, P. and Voorhes, J. J. (1992). Differential regulation of retinoic acid receptors and binding proteins in human skin. *J. Invest. Dermatol*. **98**, 673-679.

Feil, R., Brocard, J., Mascrez, B., LeMeur, M., Metzger, D. and Chambon, P. (1996). Ligand-activated site-specific recombination in mice. *Proc. Natl. Acad. Sci. USA* **93**, 10887-10890.

Feil, R., Wagner, J., Metzger, D. and Chambon, P. (1997). Regulation of Cre recombinase activity by mutated oestrogen receptor ligand-binding domains. *Biochem. Biophys. Res. Commun.* **237**, 752-757.

Feng, X., Peng, Z. H., Di, W., Li, X. Y., Rochette-Egly, C., Chambon, P., Voorhees, J. J. and Xiao, J. H. (1997). Suprabasal expression of a dominant-negative RXR alpha mutant in transgenic mouse epidermis impairs regulation of gene transcription and basal keratinocyte proliferation by RAR-selective retinoids. *Genes Dev*. **11**, 59-71.

Fisher, G. J., Talwar, H. S., Xiao, J. H., Datta, S. C., Reddy, A. P., Gaub, M. P., Rochette-Egly, C., Chambon, P. and Voorhees, J. J. (1994). Immunological identification and functional quantitation of retinoic acid and retinoid X receptor proteins in human skin. *J. Biol. Chem*. **269**, 20629-20635.

Fisher, G. J. and Voorhees, J. J. (1996). Molecular mechanisms of retinoid actions in skin. *FASEB J*. **10**, 1002-1013.

Fuchs, E. (1997). Of mice and men: genetic disorders of the cytoskeleton. *Mol. Biol. Cell* **8**, 189-203.

Ghadially, F. N. (1997). *Ultrastructural Pathology of the Cell and Matrix*, 4th edition, Vol. 2, pp. 825-872. Newton: Butterworth-Heinemann.

Giguère, V. (1999). Orphan nuclear receptors: from gene to function. *Endocr. Rev.* **20**, 689-725.

Hanley, K., Jiang, Y., Crumrine, D., Bass, N. M., Appel, R., Elias, P. M., Williams, M. L. and Feingold, K. R. (1997). Activators of the nuclear hormone receptors PPARα and FXR accelerate the development of the fetal epidermal permeability barrier. *J. Clin. Invest.* **100**, 705-712.

Hanley, K., Jiang, Y., He, S. S., Friedman, M., Elias, P. M., Bikle, D. D., Williams, M. L. and Feingold, K. R. (1998). Keratinocyte differentiation is stimulated by activators of the nuclear hormone receptor PPARα. *J. Invest. Dermatol*. **110**, 368-375.

Hanley, K., Ng, D. C., He, S. S., Lau, P., Min, K., Elias, P. M., Bikle, D. D., Mangelsdorf, D. J., Williams, M. L. and Feingold, K. R. (2000a).

Oxysterols induce differentiation in human keratinocytes and increase Ap-1-dependent involucrin transcription. *J. Invest. Dermatol*. **114**, 545-553.

Hanley, K., Kömüves, L. G., Ng, D. C., Schoonjans, K., He, S. S., Lau, P., Bikle, D. D., Williams, M. L., Elias, P. M., Auwerx, J. and Feingold, K. R. (2000b). Farnesol stimulates differentiation in epidermal keratinocytes via PPARα. *J. Biol. Chem.* **275**, 11484-11491.

Hardman, M. J., Sisi, P., Banbury, D. N. and Byrne, C. (1998). Patterned acquisition of skin barrier function during development. *Development* **125**, 1541-1552.

Hardy, M. H. (1992) The secret life of the hair follicle. *Trends Genet.* **8**, 55-61.

Hirobe T. (1995). Structure and function of melanocytes: microscopic morphology and cell biology of mouse melanocytes in the epidermis and hair follicle. *Histol. Histopathol*. **10**, 223-237.

Imakado, S., Bickenbach, J. R., Bundman, D. S., Rothnagel, J. A., Attar, P. S., Wang, X. J., Walczak, V. R., Wisniewski, S., Pote, J. and Gordon, J. S. (1995). Targeting expression of a dominant-negative retinoic acid receptor mutant in the epidermis of transgenic mice results in loss of barrier function. *Genes Dev*. **9**, 317-329.

Indra, A. K., Warot, X., Brocard, J., Bornert, J. M., Xiao, J. H., Chambon, P. and Metzger, D. (1999). Temporally-controlled site-specific mutagenesis in the basal layer of the epidermis: comparison of the recombinase activity of the tamoxifen-inducible Cre-ER^T and Cre-ER^{T2} recombinases. *Nucleic Acids Res*. **27**, 4324-4327.

Kastner, P., Grondona, J. M., Mark, M., Gansmuller, A., LeMeur, M., Decimo, D., Vonesch, J. L., Dollé, P. and Chambon, P. (1994). Genetic analysis of RXR alpha developmental function: convergence of RXR and RAR signaling pathways in heart and eye morphogenesis. *Cell* **78**, 987-1003.

Kastner, P., Mark, M. and Chambon, P. (1995). Nonsteroid nuclear receptors: what are genetic studies telling us about their role in real life? *Cell* **83**, 859-869.

Kastner, P., Mark, M., Leid, M., Gansmuller, A., Grondona, J. M., Décimo, D., Krezel, W., Dierich, A. and Chambon, P. (1996). Abnormal spermatogenesis in RXRβ mutant mice. *Genes Dev*. **10**, 80-92.

Kastner, P., Mark, M., Ghyselinck, N., Krezel, W., Dupé, V., Grondona, J. M. and Chambon, P. (1997). Genetic evidence that the retinoid signal is tranduced by heterodimeric RXR/RAR functional units during mouse development. *Development* **124**, 313-326.

Katz, S. I., Tamaki, K. and Sachs, D. H. (1979). Epidermal langerhans cells are derived from cells originating in bone marrow. *Nature* **282**, 324-326.

Kiernan, J. A. (1990) *Histological and Histochemical Methods: Theory and Practice*, 2nd edn. New York: Pergamon Press.

Kömüves, L. G., Hanley, K., Jiang, Y., Elias, P. M., Williams, M. L. and Feingold, K. R. (1998). Ligands and activators of nuclear hormone receptors regulate epidermal differentiation during fetal rat skin development. *J. Invest. Dermatol.* **111**, 429-433.

Leid, M., Kastner, P., Lyons, R., Nakshatri, H., Saunders, M., Zacharewski, T., Chen, J. Y., Staub, A., Garnier, J. M., Mader, S. and Chambon, P. (1992). Purification, cloning, and RXR identity of the HeLa cell factor with which RAR or TR heterodimerizes to bind target sequences efficiently. *Cell* **68**, 377-395.

Li, Y. C., Pirro, A. E., Amling, M., Delling, G., Baron, R., Bronson, R. and Demay, M. B. (1997) Targeted ablation of the vitamin D receptor: an animal model of vitamin D-dependent rickets type II with alopecia. *Proc. Natl. Acad. Sci. USA* **94**, 9831-9835.

Li, Y. C., Amling, M., Pirro, A. E., Priemel, M., Meuse, J., Baron, R., Delling, G. and Demay, M. B. (1998). Normalization of mineral ion homeostasis by dietary means prevents hyperparathyroidism, rickets, and osteomalacia, but not alopecia in vitamin D receptor-ablated mice. *Endocrinology* **139**, 4391-4396.

Li, M., Indra, A. K., Warot, X., Brocard, J., Messaddeq, N., Kato, S., Metzger, D. and Chambon, P. (2000). Skin abnormalities generated by temporally controlled RXRα mutations in mouse epidermis. *Nature*, 407, 633-636.

Lohnes, D., Kastner, P., Dierich, A., Mark, M., LeMeur, M. and Chambon, P., (1993). Function of retinoic acid receptor γ in the mouse. *Cell* **73**, 643-658.

Lohnes, D., Mark M., Mendelsohn, C., Dollé, P., Dierich, A., Gorry, P., Gansmuller, A. and Chambon, P. (1994). Function of the retinoic acid receptors (RARs) during development. (I) Cranofacial and skeletal abnormalities in RAR double mutants. *Development* **120**, 2723-2748.

Lufkin, T., Lohnes, D., Mark, M., Dierich, A., Gorry, P., Gaub, M. P., LeMeur, M. and Chambon P. (1993). High postnatal lethality and testis degeneration in retinoic acid receptor α mutant mice. *Proc. Natl. Acad. Sci. USA* **90**, 7225-7229.

Malloy, P. J., Pike, W. and Feldman, D. (1999). The Vitamin D receptor and the syndrome of hereditary 1,25-dihydroxyvitamin D-resistant rickets. *Endocr. Rev.* **20**, 156-188.

Mangelsdorf, D. J., Borgmeyer, U., Heyman, R. A., Zhou, J. Y., Ong, E. S., Oro, A. E., Kakizuka, A. and Evans, R. M. (1992). Characterization of three RXR genes that mediate the action of 9-cis retinoic acid. *Genes Dev*. **6**, 329-344.

Mangelsdorf, D. J., Thummel, C., Beato, M., Herrlich, P., Schutz, G., Umesono, K., Blumberg, B., Kastner, P., Mark, M. and Chambon, P. (1995). The nuclear receptor superfamily: the second decade. *Cell* **83**, 835-839.

Mascrez, B., Mark, M., Dierich, A., Ghyselinck, N. B., Kastner, P. and Chambon P. (1998). The RXRα ligand-dependent activation function 2 (AF-2) is important for mouse development. *Development* **125**, 4691-4707.

Metzger, D., Clifford, J., Chiba, H. and Chambon, P. (1995). Conditional site-specific recombination in mammalian cells using a ligand-dependent chimeric Cre recombinase. *Proc. Natl. Acad. Sci. USA* **92**, 6991-6995.

Miranda, E. P. and Granstein, R. D. (1998). Neuropeptide- and cytokine-mediated regulation of Langerhans cell function. In *Skin: Interface of a Living System* (ed. H. Tagami, J. A. Parrish and T. Ozawa), pp. 101-118. Amsterdam: Elsevier.

Nagy, A. (2000). Cre recombinase: the universal reagent for genome tailoring. *Genesis* **26**, 99-109.

Oro, A. E. and Scott, M. P. (1998). Splitting hairs: dissecting roles of signaling systems in epidermal development. *Cell* **95**, 575-578.

Panteleyev, A. A., Paus, R., Ahmad, W., Sundeberg, J. P. and Christiano, A. M. (1998). Molecular and functional aspects of the hairless (hr) gene in laboratory rodents and humans. *Exp. Dermatol*. **7**, 249-267.

Paus, R. and Cotsarelis, G. (1999). The biology of hair follicles. *New Engl. J. Med*. **341**, 491-497.

Paus, R., Stenn, K. S. and Link, R. E. (1990). Telogen skin contains an inhibitor of hair growth. *Br. J. Dermatol.* 122, 777-784.

Peters, J. M., Lee, S. S. T., Li, W., Ward, J. M., Gavrilova, O., Everett, C., Reitman, M. L., Dudson, L. D. and Gonzalez, F. J. (2000). Growth, adipose, brain, and skin alterations resulting from targeted disruption of the mouse peroxisome proliferator-activated receptor β (δ). *Mol. Cell Biol.* **20**, 5119-5128.

Porter, R. M., Reichelt, J., Lunny, D. P., Magin, T. M. and Lane, E. B. (1998). The relationship between hyperproliferation and epidermal thickening in a mouse model for BCIE. *J. Invest. Dermatol*. **110**, 951-957.

Reichrath, J., Schilli, M., Kerber, A., Bahmer, F. A., Czarnetzki, B. M. and Paus, R. (1994). Hair follicle expression of 1,25-dihydroxyvitamin D3 receptors during the murine hair cycle. *Br. J. Dermatol*. **131**, 477-482.

Reichrath, J., Munssinger, T., Kerber, A., Rochette-Egly, C., Chambon, P., Bahmer, F. A. and Baum, H. P. (1995). In situ detection of retinoid-X receptor expression in normal and psoriatic human skin. *Br. J. Dermatol.* **133**, 168-175.

Rochette-Egly, C., Lutz, Y., Pfister, V., Heyberger, S., Scheuer, I., Chambon, P. and Gaub, M. P. (1994). Detection of retinoid X receptors using specific monoclonal and polyclonal antibodies. *Biochem. Biophys. Res. Commun*. **204**, 525-536.

Roos, T. C., Jugert, F. K., Merk, H. F. and Bickers, D. R. (1998). Retinoid metabolism in the skin. *Pharmacol. Rev*. **50**, 315-333.

Sakai, Y. and Demay, M. B. (2000). Evaluation of keratinocyte proliferation and differentiation in vitamin D receptor knockout mice. *Endocrinology*. **141**, 2043-2049.

Saitou, M., Sugai, S., Tanaka, T., Shimouchi, K., Fuchs, E., Narumiya, S. and Kakizuka, A. (1995). Inhibition of skin development by targeted expression of a dominant-negative retinoic acid receptor. *Nature* **374**, 159-162.

Schlüter, C., Duchrow, M., Wohlenberg, C., Becker, M. H. G., Key, G., Flad, H.-D. and Gerdes, F. (1993). The cell proliferation-associated antigen of antibody Ki-67: a very large, ubiquitous nuclear protein with numerous repeated elements, representing a new kind of cell cycle-maintaining proteins. *J. Cell. Biol*. **123**, 513-522.

Soriano P. (1999). Generalized lacZ expression with the ROSA26 Cre reporter strain. *Nat. Genet.* **21**, 70-71.

Springer, T. A. (1990). Adhesion receptors of the immune system. *Nature* **346**, 425-434.

Sucov, H. M., Dyson, E., Gumeringer, C. L., Price, J., Chien, K. R. and

Evans, R. M. (1994). RXR alpha mutant mice establish a genetic basis for vitamin A signaling in heart morphogenesis. *Genes Dev.* **8**, 1007-1018.

Sundberg, J. P. and King, L. E. (1996). Mouse models for the study of human hair loss. *Dermatol. Clin.* **14**, 619-632.

Sundberg, J. P., Hogan M. E. and King, L. E. (1996). Normal biology and aging changes of skin and hair. In *Pathobiology of the Aging Mouse.* Vol. 2 (ed. U. Mohr, D. L. Dungworth, C. C. Capen, W. W. Carhon, J. P. Sundberg and J. M. Ward), pp. 303-323. Washington: ILSI Press.

Swiggard, W. J., Mirza, A., Nussenzweig, M. C. and Steinman, R. M. (1995). DEC-205, a 205-kDa protein abundant on mouse dendritic cells and thymic epithelium that is detected by the monoclonal antibody NLDC-145: purification, characterization, and N-terminal amino acid sequence. *Cell Immunol.* **165**, 302-311.

Vasioukhin, V., Degenstein, L., Wise, B. and Fuchs, E. (1999). The magical touch: genome targeting in epidermal stem cells induced by tamoxifen application to mouse skin. *Proc. Natl. Acad. Sci. USA* **96**, 8551-8556.

Vassar, R., Rosenberg, M., Ross, S., Tyner, A. and Fuchs, E. (1989). Tissue-specific and differentiation-specific expression of a human K14 keratin gene in transgenic mice. *Proc. Natl. Acad. Sci. USA* **86**, 1563-1567.

Wan Y-J. Y., An, D., Cai, Y., Repa, J. J., Chen, T. H. P., Flores, M., Postic, M., Magnuson, M. A., Chen, J., Chien, K. R. et al. (2000). Hepatocyte-specific mutation establishes retinoid X receptor α as a heterodimeric integrator of multiple physiological processes in the liver. *Mol. Cell Biol.* **20**, 4436-4444.

Wang, X., Zinkel, S., Polonsky, K. and Fuchs, E. (1997). Transgenic studies with a keratin promoter-driven growth hormone transgene: prospects for gene therapy. *Proc. Natl. Acad. Sci. USA* **94**, 219-226.

Wendling, O., Chambon, P. and Mark, M. (1999). Retinoid X receptors are essential for early mouse development and placentogenesis. *Proc. Natl. Acad. Sci. USA* **96**, 547-551.

Xiao, J. H., Feng, X., Di, W., Peng, Z. H., Li, L. A., Chambon, P. and Voorhees, J. J. (1999). Identification of heparin-binding EGF-like growth factor as a target in intercellular regulation of epidermal basal cell growth by suprabasal retinoic acid receptors. *EMBO J.* **18**, 1539-1548.

Yen, P. M., Liu, Y., Sugawara, A. and Chin, W. W. (1996) Vitamin D receptors repress basal transcription and exert dominant negative activity on triiodothyronine-mediated transcriptional activity. *J. Biol. Chem.* **271**, 10910-10916.

Yoshizawa, T., Handa, Y., Uematsu, Y., Takeda, S., Sekine, K., Yoshihara, Y., Kawakami, T., Arioka, K., Sato, H., Uchiyama, Y. et al. (1997). Mice lacking the vitamin D receptor exhibit impaired bone formation, uterine hypoplasia and growth retardation after weaning. *Nat. Genet.* **16**, 391-396.